DEUTSCHES ELEKTRONEN-SYNCHROTRON

DESY 95-013
February 1995

Study of $D^*(2010)^{\pm}$ Production in ep Collisions at HERA

ZEUS Collaboration

ISSN 0418-9833

NOTKESTRASSE 85 - 22603 HAMBURG

To be sure that your preprints are promptly included in the HIGH ENERGY PHYSICS INDEX, send them to (if possible by air mail):

DESY
Bibliothek
Notkestraße 85
22603 Hamburg
Germany

DESY-IfH
Bibliothek
Platanenallee 6
15738 Zeuthen
Germany

DEUTSCHES ELEKTRONEN-SYNCHROTRON

DESY 94–239
December 1994

On the Quark-Antiquark Potential at Short Distances

P. Altevogt

Institute for Supercomputing and Applied Mathematics, IBM, Heidelberg

F. Gutbrod

Deutsches Elektronen-Synchrotron DESY, Hamburg

ISSN 0418-9833

NOTKESTRASSE 85 - 22603 HAMBURG

To be sure that your preprints are promptly included in the HIGH ENERGY PHYSICS INDEX, send them to (if possible by air mail):

DESY
Bibliothek
Notkestraße 85
22603 Hamburg
Germany

DESY-IfH
Bibliothek
Platanenallee 6
15738 Zeuthen
Germany

DESY 94-239
December 1994

ISSN 0418-9833

On the Quark-Antiquark Potential at Short Distances

P. Altevogt
Institute for Supercomputing and Applied Mathematics, IBM, Heidelberg
and
F. Gutbrod
Deutsches Elektronen-Synchrotron DESY, Hamburg

Abstract

We investigate the static quark-antiquark potential up to distances of 8 lattice units for pure SU(2) gauge theory on lattices with anisotropic couplings. The action is the Wilson action with a coupling for time-like plaquettes which differs from those for space-like ones. Numerical simulations are performed in a large range of β. The potential is obtained by fitting 'cooled' Wilson loops with up to 4 exponential terms. An interpolation of the potentials by a sum of a perturbative term, a linear term and by lattice artifacts shows poor scaling in comparison with the isotropic case. If the coupling in the time-like region is reduced, the linear term is much smaller than in the isotropic case, and vice versa. Consequences for the bag picture for hadrons are discussed.

1 Introduction

The potential between static charges in non-abelian gauge theories is a physical quantity of considerable interest. This holds, of course, especially for the region where the potential is rising almost linearly, since the linear rise is of crucial importance for the understanding of quark confinement. But also the details in the transition region towards the short range, Coulomb-like behaviour may have phenomenological implications e.g. on the spectra of heavy quarkonia, and they are relevant for fundamental questions. One of those is whether the linear contribution extends down to small distances, like in bag models [1, 2, 3, 4] and in a phenomenological parametrization of the potential [5], or whether there the perturbative expansion converges, at least in a practical sense. The first case could be realized in such a way that the perturbative expansion in the renormalized, running coupling constant is asymptotically converging, and that terms decreasing exponentially fast in the inverse coupling constant are numerically non-negligible even in the continuum limit.

The potential in this region can be calculated, with small errors, by Monte Carlo lattice simulations. Especially for the case of pure gauge theory and for SU(2), a remarkable statistical accuracy can be achieved. The simulations performed so far [6, 7, 8] have clearly demonstrated the dominance of a linear term at large distances, i.e. where the perturbative expansion makes no sense, and of the Coulomb-like potential, with a running coupling constant, at small distances. A linear term seems to persist down to small distances, but its magnitude is, to some extent, a matter of parametrization. Its phenomenological implications in the transition region are perhaps not too dramatic. Anticipating the lattice results to be described below, the non-perturbative term contributes to the quark-antiquark force by about 15% at a distance of 0.25 fm, with an increasing trend towards larger distances.

The variation of the potential as a function of the bare lattice coupling constant g_0^2 poses certain difficulties for a convincing interpretation. The results of all simulations agree in so far that this variation does not follow the predictions of two-loop perturbation theory[1]. The departure can be a consequence of the fact that if we consider the renormalized, running coupling constant $\alpha(R)$, including two-loop corrections, as expansion parameter for the perturbative series, the parameter is not small compared to unity in the region of interest. This hold at least for separations of the charges $R/a > 3$ say at intermediate values of g_0^2 (a is the lattice constant). This large expansion parameter could well lead to a scale differing from the perturbative one. Another, more radical interpretation could be that the linear contribution in the transition region is a lattice artifact which vanishes in the continuum limit $g_0^2 \to 0$.

The magnitude and the g_0^2-dependence of a non-analytic term can of course be studied directly for Creutz ratios, χ_l, without the need for complicated extrapolation procedures as for the potential (see section 4 in this context). It has been shown in [8] that many χ_l, including those with a geometry l closely related to the potential, can easily be represented[2] by few terms in $\alpha(l)$, if a non-perturbative term $\chi_{l,np}$ is added, with a typical variation

$$\chi_{l,np} \sim exp(-\gamma_l/g_0^2), \tag{1}$$

where γ_l depends on the geometry l of the Creutz ratio under consideration. The l-dependence of such terms is consistent with an area term, but the factor γ_l turned out to be inconsistent with this interpretation, being too large for all ratios, and pointing again towards a vanishing of $\chi_{l,np}$ in the continuum limit.

It is quite difficult to test the hypothesis of a decreasing linear term in the potential by further lowering g_0^2, because of the necessity to increase the lattice volume proportionally to the exponentially increasing lattice scale and, even more demanding, to measure the potential at an increasing distance. Therefore, other methods to study systematic effects on the lattice will be helpful. In this paper we will present the results of lattice simulations in pure SU(2) gauge theory based on an action different from the standard Wilson action. We consider lattices with different scales in space-like and in time-like directions, obtained technically by multiplying the contribution to the action of those plaquettes with one time-like link by a different factor as the space-like plaquettes. In the isotropic case this factor is $\beta = 4/g_0^2$ and here we take

$$\beta_t = \xi^2 \beta. \tag{2}$$

The action, written in a way to indicate necessary scale transformations, is then

$$S = \xi\beta\,(\frac{1}{\xi}\sum_{space} + \xi\sum_{time})\frac{tr}{2}(1 - \prod_{plaq} U_i). \tag{3}$$

On the classiceal level, the ξ-factors in front of the sums will be removed by scale- and gauge field transformations along the time directions, and the leading ξ-factor by a change in the coupling constant. For $\xi \to \infty$ we approach the Hamiltonian limit of a continuous time variable[3]. Based on the perturbative study of the static potential, to

[1] This is called a departure from asymptotic scaling.

[2] Formally, expansions in the running coupling $\alpha(l)$ are always possible in view of finite errors of the Monte Carlo data, but at the expense of large and oscillating higher order coefficients.

[3] Anisotropic lattices have been studied previously mainly in connection with Monte Carlo simulations at finite temperature [9, 10] where the finer granularity in the time-direction is helpful.

be discussed in the next section, the potential will then be derived from the usual Wilson loops $W(R,T)$ via

$$aV(R) = -\xi \lim_{T\to\infty} \frac{1}{a} ln \frac{W(R,T)}{W(R,T-a)}. \quad (4)$$

Here a and $V(R)$ can be taken either in lattice units or in physical units.

Qualitatively, in the case of $\xi > 1$, the effect of such a change on the lattice gauge fields will be a reduction of the field fluctuations along the time direction. This reduction will of course couple back to the spatial directions, and in order to obtain the same physics as in the isotropic case, one has to consider a bare coupling constant differing from g_0^2, both by a ξ-dependent factor[4] and by an additive shift to the inverse coupling. The latter operation is equivalent to a multiplicative change in the connection of the scale parameter for a physical quantity, (here, for the potential, Λ_R) and the lattice scale parameter Λ_{latt}. These transformations are calculable in 1-loop perturbation theory. With their help it should be possible to absorb the anisotropy effects into ξ-dependent scale factors not deviating too strongly from the perturbative ones. The Monte Carlo data to be presented here show that this is not the case. If we calculate a perturbative contribution to the potential with a running coupling constant based on the perturbative scale parameters and include a second order contribution with a free coefficient, the data require, without doubt, the inclusion of a linear non-perturbative term. This linear contribution can be determined independently from a fit to the R-behaviour of the potential at fixed β or from the β-behaviour at fixed R, with similar results. The scale-dependence of the linear term, however, differs from that of the perturbative term, and, more importantly, it is strongly ξ-dependent. Especially, for $\xi < 1$, we find a strong reduction as compared to the isotropic case. A speculative explanation is that in this case one encounters a strong suppression of negative plaquette values in space-like directions, and we believe this case to be closer to the continuum case as the case $\xi > 1$. A possible and simple conclusion is that the linear term, which shows up in most numerical analyses of lattice data, is a lattice artifact and that it may vanish in the continuum limit.

Indications for such violations of scaling are not easily visible from a direct comparison of potentials belonging to different actions since the discreteness of the lattice is very disturbing if the scale parameters do not match perfectly. In order to overcome this, we have to interpolate the Monte Carlo data, and to correct for the effects of finite lattice spacing at small R/a. There perturbation theory will be a good guide, and we will describe the perturbative expansion of the potential in the next section. More details will be given in appendix A. For moderate R/a, there is no well founded interpolation formula especially for the transition between the perturbative regime and the confining one. In section 3 we argue in favour for a simple addition of a perturbative and of a linear term.

The Monte-Carlo data and the results from the interpolation procedure will be described in section 4, and section 5 contains a discussion and conclusions.

The data have been taken on a variety of parallel computers, and in appendix B we will shortly indicate the methods of parallelization and report on the performance achieved.

[4] This will then allow to use the standard renormalization group connection between the bare coupling and the renormalized one

2 Perturbation Theory on Anisotropic Lattices

2.1 Overview

The perturbative expansion of the potential, up to one-loop accuracy, will fix the rescaling of the potential (4), the rescaling of the coupling constant and of the Λ-parameters for anisotropic lattices, and it will give information on the lattice artifacts at small R/a beyond the tree level. For this purpose the formulas given by [11, 12] will be generalized. We start from the action (3) and expand with respect to $g_0^2 = 4/\beta$. After a rescaling of time-like gauge fields on an anisotropic lattice of size $V_\xi = \xi L \times L^3$ we obtain, for $L \to \infty$, the classical action in momentum space:

$$S_0 = \frac{1}{2} \int_{-\pi}^{+\pi} \frac{dk^4}{(2\pi)^4} \sum_{\mu=0,3} A_\mu(k) A_\mu(-k) [\xi^2 \widehat{k_0}^2 + \sum_{i=1,3} \hat{k_i}^2)], \quad (5)$$

where $\hat{k_i} = 2 \sin k_i'/2$, and the last bracket in (5) is the inverse anisotropic propagator, $D_\xi^{-1}(k)$. The details of the intermediate steps, including gauge fixing, are given in appendix A.

In order to obtain a closer connection to the isotropic case, one can transform the dk_0-integration and introduce a bare propagator $D_\xi'(k)$ by the substitution:

$$\int_{-\pi}^{\pi} dk_0 / (\xi^2 \widehat{k_0}^2 + \sum_{i=1,3} \hat{k_i}^2) = \xi^{-1} \int_{-\xi\pi}^{\xi\pi} dk_0 D_\xi'(k), \quad (6)$$

with

$$D_\xi'(k) = 1/(\xi^2 \widehat{k_0/\xi}^2 + \sum_{i=1,3} \hat{k_i}^2). \quad (7)$$

This propagator deviates from the isotropic one starting in $\mathcal{O}(\widehat{k_0}^4)$. The contributions to the one-loop approximation to the the potential are the following [11, 12]:

1. The Wilson-loop expansion,
2. the triple-gluon coupling,
3. the quadruple-gluon coupling,
4. the Fadeev-Popov determinant,
5. the measure contribution,

The spider graph, which contributes to Wilson loops, vanishes for the potential, when Feynman gauge is employed. We will list the individual terms in the appendix.

For a basic understanding, one has to identify the influence of the anisotropy on the tree level potential, next on those terms of the one-loop potential proportional to the tree level, and especially of the logarithmic corrections on one-loop level. This will be done both in momentum- and in x-space. The summary of the results is that the anisotropy will modify the Wilson loops, for fixed g_0^2 and in the limit of large R and T, or the potential at small momenta, in the following way:

1. On tree level, the Wilson loops will be multiplied by a factor ξ^{-2}.
2. On one-loop level, the terms proportional to tree level will be modified by a complicated $\xi-$dependent factor, which has to be evaluated numerically.
3. Also on one-loop level, the terms logarithmic in R will be multiplied by a factor ξ^{-3}.

These factors can be eliminated by the following redefinitions and scale transformations:

1. From the factor ξ^{-2} on tree level, one ξ^{-1} will be absorbed by the anisotropic connection between the Wilson loops and the physical potential (see eq. (4)).
2. Another factor ξ^{-1} will be absorbed into the bare squared coupling constant.

$$g_0^2 - g_0'^2 = \frac{g_0^2}{\xi}. \tag{8}$$

   Thus, the logarithmic terms expressed in $O(g_0'^4)$ experience no further modification.
3. The complicated modifications of the terms in $O(g_0^4)$ proportional to the tree-level potential will be absorbed into a redefinition of the connection of the parameter Λ_R and the lattice parameter Λ_{latt} where the latter is expressed in the usual form, but as function of $g_0'^2$ (see (12)).

2.2 Results

To consider only the momentum space representation of the one-loop integrals given in appendix A, eqs. (46, 47 etc.), is of course much simpler than to evaluate those intergrals completely in R-space. Especially the Λ_q−parameter for the potential in momentum space can be accurately obtained by taking the limit $\vec{q}^2 \to 0$ and comparing the numerical result with the expression of the continuum in order g_0^4,

$$V_{1-loop}(q) = \xi^{-2} C_r \frac{g_0^4 \beta_0}{q^2} \ln \frac{q^2}{\Lambda_q^2} = C_r \frac{g_0'^4 \beta_0}{q^2} \ln \frac{q^2}{\Lambda_q^2}, \tag{9}$$

with

$$C_r = \frac{N^2-1}{2N}, \quad \beta_0 = \frac{11N}{48\pi^2}, \tag{10}$$

and $N=$ number of colours. Thus, the numerical evaluation of the integrals over k of (46,48 to 60), keeping $\vec{q}$ fixed, yields the parameter Λ_q, and this gives, after conversion to R-space, for $\xi^2 \neq 1$,

$$\Lambda_{\xi,R} = \begin{cases} 49.86\, \Lambda_{latt}, & \xi^2 = 3/2 \\ 67.64\, \Lambda_{latt}, & \xi^2 = 2/3 \end{cases} \tag{11}$$

with a lattice parameter Λ_{latt} depending on the modified coupling constant (8),

$$\Lambda_{latt} = a^{-1} (\beta_0 g_0'^2)^{-\beta_1/2\beta_0^2} exp(-1/2\beta_0 g_0'^2), \tag{12}$$

with

$$\beta_1 = 136/3(4\pi)^4. \tag{13}$$

For the force parameter $\Lambda_F$we obtain [13, 14]

$$\Lambda_{\xi,F} = \begin{cases} 18.33\, \Lambda_{latt}, & \xi^2 = 3/2 \\ 24.88\, \Lambda_{latt}, & \xi^2 = 2/3 \end{cases} \tag{14}$$

to be compared with the isotropic case [13, 14]

$$\Lambda_{\xi=1,F} = 20.77 \Lambda_{latt}. \tag{15}$$

We will use these values for the specification of the perturbative potential, to be presented in section 3, apart from the lattice artifacts.

In what follows, the suffix ξ will be dropped again for the Λ−parameters.

2.3 Lattice Artifacts

The tree level artifacts are unchanged with respect to the isotropic case ($\xi = 1$) apart from the normalizing factor ξ. To obtain the one-loop corrections, we have to insert the Λ_R−parameter, determined previously, into the continuum formula (9) and compare it now, at fixed R, to the full 7-dimensional integrals (46 to 60), specified in the appendix. The main result is that

- the artifacts in 1-loop order do not follow closely the pattern of the tree level, but are enhanced for $R/a \geq 2$ as compared to $R/a = 1$,
- there is an inceasing trend, in the order of 10%, in the artifacts between $\xi^2 = 3/2$ and $\xi^2 = 2/3$.

In later applications, we will use an expansion of the artifacts with respect to the bare coupling constant:

$$V_{corr}(R) = -\frac{C_r}{R} \frac{g_0'^2}{4\pi} (a_1(R) + a_2(R) g_0'^2 + a_3(R) g_0'^4), \tag{16}$$

where $a_3(R)$ is unknown. We will fit it to the most exact Monte Carlo data at large β, where the contribution from the linear term is negligible (assuming asymptotic scaling). This is done for $\xi^2 \neq 1$ only, since for $\xi^2 = 1$ such large β-values are not available. There, $a_3(R)$ is obtained by linear interpolation. The tree level terms $a_1(R)$, the 1-loop results $a_2(R)$ and the fit results for $a_3(R)$ are given in table 1.

		$\xi^2 = 3/2$		$\xi^2 = 1$		$\xi^2 = 2/3$	
R/a	$a_1(R)$	$a_2(R)$	$a_3(R)$	$a_2(R)$	$a_3(R)$	$a_2(R)$	$a_3(R)$
1	0.081	0.0150	0.0040	0.0156	0.0050	0.0163	0.0060
2	0.077	0.0169	0.0088	0.0181	0.0100	0.0195	0.0115
3	0.038	0.0079	0.0025	0.0085	0.0033	0.0093	0.0040
4	0.019	0.0038	0.0020	0.0042	0.0025	0.0045	0.0030
5	0.011	0.0021	0.0008	0.0023	0.0012	0.0025	0.0016
6	0.007	0.0013	0.0	0.0013	0.0	0.0014	0.00

Table 1: Display of lattice artifacts, normalized by the Coulomb potential.

It is clear from the 1-loop results in table 1 that the expansion (16) is not necessarily converging well for $g'^2 = \mathcal{O}(1)$, similarly as the potential itself. Since the shape of the corrections, as in functions of R, varies from order to order, a straightforward use of the renormalized coupling instead of the bare one seems to be unjustified. It should be noted, however, that the contribution from $a_3(R)$ is larger than the errors of the Monte Carlo data only by a factor 10 or less, so a careful treatment of this term is not necessary.

Of course, there is considerable uncertainty against a simultaneous variation of the perturbative parameters, especially of a necessary higher order coefficient c_2 (see eq. (18) below), and of the lattice artifacts. In section 4 we will return to this problem and study the window in which both quantities can be varied without violating some side conditions, among others the β-variation of the higher order coefficient and the β-variation of the linear term. It will turn out that the main result of this paper, namely the strong dependence of the linear term on ξ, is unchanged if the parameters are varied within this window.

3 On the Description and Interpolation of Lattice Results

Both for a check of scaling properties and for the separation of perturbative and non-perturbative terms, an interpolation of the lattice data is necessary. Unfortunately, interpolation formulae are ad hoc, given the present lack of understanding, and we can only give a few heuristic arguments for or against special parametrizations.

A central question is whether we insist on describing the lattice potential $V(R/a)$ (or the lattice force, i.e. the finite differences of the potential), in terms of an effective running coupling constant $\alpha_{eff}(R)$ plus a lattice artifact correction at small R/a (see [15, 16, 17, 18]). Our experience is that this does not work if we take $\alpha_{eff}(R/a)$ to be close to the perturbatively renormalized coupling constant (defined below in (19)). The reason is connected with the very precise Monte Carlo force at small R, which rises with decreasing β more rapidely than allowed by a low order polynomial with decreasing coefficients.

An alternative route, which takes into account the latter effect, is to explicitly add a term which is non-analytic at $g_0^2 = 0$, e.g. a term $\sim e^{-\gamma/g_0^2}$. Then the running coupling constant $\alpha(R)$ can easily be connected with g_0^2 by the standard renormalization group procedure. It has been shown recently by direct computation of the renormalized couplings [19, 20] that this is possible provided the scales are chosen correctly. The incorporation of a non-perturbative term has been advocated recently in [21], albeit with the full string tension and not with a reduced one, as we will propose below.

A third possibility is to define an expansion parameter directly by some Monte Carlo data, most easily by the average plaquette value [22]. In this way non-analytic terms are included, to some extent, in the expansion parameter.

We first describe the second route, which we will use in this analysis.

3.1 Lattice Perturbation Series Plus String Tension

Of course the inclusion of a non-analytic term into the ansatz for the potential is only sensible if the term has a simple structure in R or in momentum space. Here we assume that it is to a good approximation linear in R, which means that in Fourier space it is concentrated at very small momenta.

The perturbative lattice potential (apart from small R/a-corrections) will be written as a second order polynomial in the R-dependent coupling $\alpha(R)$, by integrating the force,

$$V_p(R) = V_0 + \int_{R_c}^{R} dR' F_p(R'), \tag{17}$$

with

$$F_p(R) = \frac{C_R}{R^2}\,\alpha(R)\,(1 + c_2\alpha(R)). \tag{18}$$

We take the running coupling constant in two-loop approximation

$$\alpha(R) = \left[4\pi\{-\beta_0 \ln R^2\Lambda_F^2 + \frac{\beta_1}{\beta_0}\ln(-\ln R^2\Lambda_F^2)\}\right]^{-1}, \quad \beta_1 = 136/3(4\pi)^4. \tag{19}$$

The second order coefficient, c_2, will be fitted to the data at each β individually, and it should come out rather as a constant. The scale parameter for the force, Λ_F, is related to the lattice scale parameter Λ_{latt} as given in eq. (14).

Before we can discuss a possible modification of (19) at large R, where $\alpha(R)$ becomes singular, the confining force has to be specified. A working model for confinement may

be the nonlinear version of Maxwell's theory proposed by Adler [3, 4]. The essential content of such models is that the vacuum does not support weak fields originating from static charges. The field configuration around a dipole charge will have a perturbative region with strong fields, and a vacuum region with zero fields. The transition takes place where the electric field strength $|\vec{E}|$ drops to a critical value E_0. This occurs at a distance r_c from the center between the charges

$$r_c \sim (eR/E_0)^{1/3}, \tag{20}$$

where e is the charge and R the separation of the charges. The perturbative field energy outside r_c is

$$V_c(R) \sim \frac{e^2R^2}{r_c^3} \sim eE_0R. \tag{21}$$

Without posessing a more detailed picture, the most natural assumption is that it is this fraction of the total field energy which is modified by confinement, in the sense of a redistribution of the electric flux lines. This will lead most likely to a modification of (21) by a constant numerical factor. We thus get a modification of the Coulomb potential by a term linear in the separation of the charges. The same principal result is obtained in the bag model [1, 2], although with a somewhat different argumentation.

We thus assume that a quantitatively reasonable fit to the static potential can be obtained by the ansatz

$$V(R) = V_p(R) + V_{corr}(R) + K_rR, \tag{22}$$

where $V_{corr}(R)$ are the lattice artifact corrections, which are relevant only for $R/a \leq 4$. This ansatz contains the parameters V_0, c_2 and K_r, which will be determined independently for all β. The potential is scale invariant, if $K_r \propto \Lambda_F^2$ (see eq. (14)), i.e. if K_r is non-analytic in g_0^2. We call K_r the **reduced** string tension, since it will be most likely smaller that the full string tension, according to the following argument.

The representation (22) becomes meaningless for increasing R -at the latest- at the point where the perturbative potential V_p increases stronger than linearly, a behaviour which is theoretically inconsistent with the transfer-matrix property of Wilson loops. The latter does not allow a faster than exponential decrease, with positive coefficients, of Wilson loops $W(R,T)$ both for R fixed, $T \to \infty$, and vice versa. An exponential decrease of the form $exp(-\gamma RT)$ is therefore the strongest decrease allowed. A working assumption is then to continue the perturbative potential linearly starting from the point where the renormalization group-improved potential becomes linear anyhow. One thus would interpret the sum of the linear continuation and K_r as the physcal string tension.

In the analysis to be presented here we will not use values of R beyond the point where the slope of the perturbative force changes sign. This occurs, for β=2.2 and $\xi^2 = 3/2$, at $R/a \approx 10$. Of course this value is dangerously close to the maximal value $R/a = 8$ used in the analysis, but due to the larger errors for the last pont, its influence on the fits is quite limited. Omitting it from the fit does not change the results by more than half a standard deviation.

3.2 Using an Effective Coupling Constant

An alternative interpretation of numerical lattice data on the potential is in terms of an effective running coupling constant $\alpha_{eff}(R)$ [15, 16, 17, 18] . There the complete

lattice force $F(R)$ is written, apart from lattice artifacts, as a generalized Coulomb term:

$$F(R) = \frac{C_R}{R^2}\alpha_{eff}(R). \tag{23}$$

This representation even can be used, after Fourier transforming, to describe the confining region by introducing a pole of the coupling constant at $q^2 = 0$:

$$\alpha_{eff}(q^2) \sim \frac{1}{q^2}. \tag{24}$$

Formally, such a representation is always possible, and it will lead to an accurate determination of $\alpha_{eff}(R)$. If the assumption made in the previous subsection about the existence of a non-perturbative linear force is correct, the latter is to be incorporated in the coupling constant[5]. After the coupling constant has been derived from the force, one requires the determination of a scale parameter at every β-value. This can be done from the Monte Carlo data for the string tension [15, 17, 18] or for the average plaquette value [22]. Since also the latter may have a non-analytic contribution, a significant part of this can be incorporated into the expansion parameter. This leads to a definite, but not complete reduction of the departures from asymptotic scaling [23]. The distribution of plaquette values P extends, at present β, well below $P = 0$, and suppressing the negative plaquette values in the action changes scales significantly [24]. We therefore hesitate to attribute a universal significance to such contributions.

4 Monte Carlo Data and Results

4.1 The Lattices

Monte Carlo simulations have been performed on a variety of MIMD-parallel computers with distributed memory. Some implementation- and performance details will be given in appendix B and in references quoted there. We update the lattice in a checkerboard sequence, with a mixture of heatbath and overrelaxation steps in the ratio 1:8. Data have been taken on various anisotropic lattices at β-values and lattice sizes as given in table 1. For the data sets with $\xi \neq 1$, the boundary conditions were periodic in the long time direction, and twisted in the spatial directions [25], i.e.

$$U_\mu(t, x + L_x, y, z) = \tau_x U_\mu(t, x, y, z)\tau_x, \tag{25}$$

and similarly for y and z, where the SU(2)-matrices U_μ are taken in the Pauli-representation. It is known that this trick reduces the finite volume errors in Creutz ratios considerably. The data sets #21 and #23 (the latter is from [6]) use periodic boundary conditions, whereas for #22 the twist is for the short directions only. Planar Wilson loops[6] will be derived from a cooled configuration, obtained by repeated substitution

$$U_\mu(x) \to \mathcal{P}_{SU2}[2 \times U_\mu(x) + V_{\mu,s}(x)],\ \mu = x, y, z, \tag{26}$$

where the potential $V_{\mu,s}(x)$ is constructed out of the U_μ on spatial plaquettes only. The symbol $\mathcal{P}_{SU(2)}$ in (26) means normalization onto SU(2)-matrices. For several data sets,

[5] We regard it as an open question whether α_{eff} determined in this way is useful as a general purpose expansion parameter.

[6] It is well known that additional information, especially on lattice artifacts are contained in non-planar Wilson loops. The authors found it not so easy to parallelize the whole evaluation package with sufficient flexibility, such that this additional information got lost.

β	# of set	ξ^2	lattice size	number of sweeps	size of loops
2.2	1	3/2	$24^3 \times 64$	70.000	8×12
	2		$48^3 \times 80$	12.100	12×16
2.3	3		$12^3 \times 32$	17.700	6×10
	4		$24^3 \times 64$	118.000	8×12
2.4	5		$12^3 \times 32$	56.500	8×10
	6		$24^3 \times 64$	60.000	8×12
2.5	7		$24^3 \times 64$	61.000	8×12
	8		$32^3 \times 128$	13.000	8×12
2.6	9		$24^3 \times 64$	29.000	8×12
2.7	10		$12^3 \times 32$	28.000	8×12
	11		$24^3 \times 64$	40.000	8×10
	12		$24^3 \times 64$	10.000	8×10
2.8	13		$32^3 \times 64$	29.000	8×12
	14		$48^3 \times 80$	20.000	12×16
2.9	15		$24^3 \times 64$	64.000	8×12
3.3	16	2/3	$24^3 \times 64$	22.000	8×12
3.4	17		$24^3 \times 64$	10.000	8×12
3.8	18		$24^3 \times 64$	14.000	8×12
	19		$32^3 \times 128$	16.000	8×12
5.0	20		$48^3 \times 32$	3.000	8×12
2.7	21	1.0	24^4	50.000	10×12
2.8	22		$24^2 \times 32^2$	110.000	12×12
2.85	23		$48^3 \times 56$	$\sim 10^5$	see [6]

Table 2: Overview over new lattice data on anisotropic lattices and on older ones on isotropic lattices.

the time-like gauge fields have been 'improved' by the multihit method [26], using the uncooled time-like gauge fields.

As an preliminary information on the potential (4), the T-dependent potential approximants

$$aV(R, T) = -\ln W_c(R, T)/W_c(R, T-1) \tag{27}$$

are useful. The typical relative accuracy of these quantities ranges from $5 \cdot 10^{-4}$ at $R = 8, T = 12$ and $\beta = 2.2$ to $2.5 \cdot 10^{-4}$ with the same space-time points at $\beta = 2.8$. There is still a noticable drop of the approximants for growing T, such that a numerical extrapolation to $T \to \infty$ is necessary. For this purpose, the cooled Wilson loops will be represented by a sum of exponentials,

$$W_c(R, T) = \sum_{i=0,3} \lambda_i(R) e^{-m_i(R)T}. \tag{28}$$

The smallest mass, called $m_0(R)$, will be identified with the potential, including the renormalization factor ξ:

$$aV(R) = \xi m_0(R). \tag{29}$$

Fits with the ansatz (28) have been made in the range $T_0 \geq T \geq 12$ with T_0 varying between[7] 0 and 6. For a 3-mass fit, the potential $V(R)$ shows a plateau for $T_0 = 1 \cdots 3$, within the statistical errors which were determined at T_0=3. The value for m_0 agrees

[7] Wilson loops with time-extension 0 are simply = 1.

with that obtained from a 4-mass fit with T_0=0. For higher values of T_0, the fit becomes unstable and $\lambda_3(R)$ may be zero. There is a slight trend for the potential determined from $T_0 = 1$ to ly above those determined from higher T_0-values, but this effect is in the relative order of $1 \cdot 10^{-3}$. For a 2-mass fit, there is a clear decrease of $m_0(R)$ starting from $T_0 = 1$ to $T_0 = 4$, where in most cases a plateau is reached which agrees with that of the 3-mass fit.

The errors of $V(R)$ have been determined by the jackknife method, using around 20 bins. Since the number of cooling steps is different for the various data sets, the fits have been performed for the data sets individually. Since among most of those no significant discrepancy has been observed, the results for the potential have been averaged. Within the errors of the extrapolation, no dependence of $V(R)$ on the lattice size has been observed, except at β= 2.7 among the data sets #11 and #12, which is a 3 s.d. effect for all R. The set #12 has exceptionally small errors, and the most likely explanation is that there we observe a 'freezing', i.e. the lattice has been caught in a twisted configuration. We have averaged the potentials and added half of the difference as a systematic error to the statistical ones. Although the resulting error is still very small ($\mathcal{O}(1 \cdot 10^{-4})$) for small R, it is evident that more work on finite lattice size effects is needed.

4.2 Results

The potentials obtained as described above have been fitted by the ansatz (22). This fit contains 3 parameters, and it is for 8 points in R. In figs. 1, 2 and 3 we display the differences between the fit (22) and the Monte Carlo data for several values of β and ξ. In order to get a feeling for the quality of the fit, one has to note that the lattice forces (18) are around $a^2F(R) = 0.10$ at $R = 1$, β= 2.2, and $a^2F(R) = 0.060$ at $R = 1$, β= 2.9. The relative deviations from the fits are thus in the order of 10^{-3} or less.

It is evident from the figures that the fits are somewhat too good, implying that the errors are overestimated. This is reasonable since the correlations between adjacent R-values are not properly taken into account. Even when reducing the errors considerably, there is no trend of a systematic deviation. In table 3 we show, for each β, the resulting fit parameters and $\chi^2/d.f.$. The latter is somewhat too small, in accordance with the impression gained from the figures.

Next we note that the second order coefficient in (18), c_2, comes out with a weakly decreasing trend for increasing β, whereas a totally satisfactory solution to the interpolation problem would require c_2 to be a constant for all values of ξ and β. In order to express the drop of c_2 in terms of an effective coupling constant, we note that it is in the order of 0.16, and that $\alpha(R)$ is smaller than 0.5 except for the last 2 R-values at β= 2.2. We conclude that this trend amounts to a drift of less than 8% in the perturbative force, the total variation being a factor 3. This may be accounted for by a slight departure from the two-loop evolution equation, which shows up also in the determination of the running coupling constant on physically small lattices [20]. We have checked that c_2 can be made constant by a smooth departure of the β-function from the two-loop scaling formula (12) by about 7% in the range $2.2 \leq \beta \leq 2.9$, in which the scale varies by a factor 10. Such a contribution from higher orders to the β-function is certainly not alarming. The fact, that c_2 is also slightly ξ-dependent implies that the small corrections to the β-functions are non-universal.

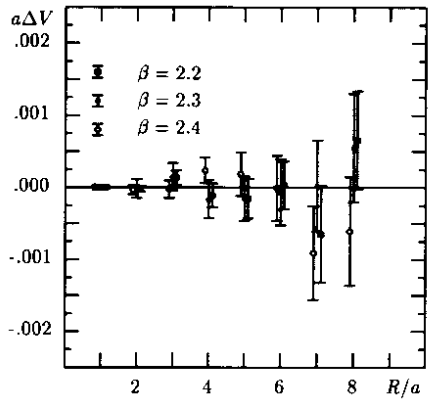

Figure 1: Differences between potentials and fits for β = 2.2, 2.3 and 2.4, ξ^2 = 3/2.

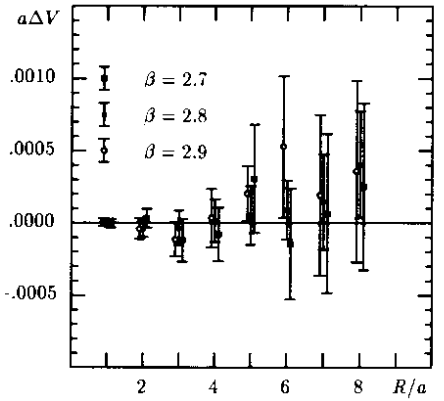

Figure 2: Differences between potential and fits for β = 2.7, 2.8 and 2.9, ξ^2 = 3/2.

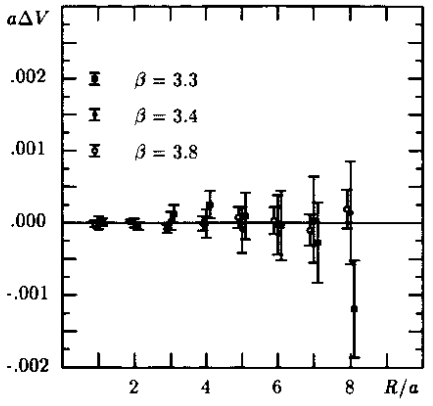

Figure 3: Differences between potential and fits for $\beta = 3.3, 3.4$ and 3.8, $\xi^2 = 2/3$.

β	set#	ξ^2	c_2	a^2K_r	Λ_F	K_r/Λ_F^2	$\chi^2/d.f.$
2.2	1+2	3/2	0.473(6)	0.0062(1)	0.04008	3.85(7)	0.9
2.3	4		0.438(15)	0.0031(2)	0.02937	3.62(20)	0.4
2.4	6		0.423(11)	0.0016(1)	0.02151	3.53(27)	1.0
2.5	7+8		0.399(11)	0.00084(5)	0.01573	3.4(2)	0.4
2.6	9		0.356(14)	0.00057(7)	0.01150	4.3(5)	0.5
2.7	11+12		0.331(14)	0.00038(11)	0.00841	5.4(1.5)	0.4
2.8	13+14		0.336(4)	0.00012(5)	0.00614	5.1(1.8)	-
2.9	15		0.314(20)	0.00007(12)	0.00448	1.3(9.0)	0.5
3.3	16	2/3	0.358(6)	0.0029(1)	0.05444	0.98(5)	1.5
3.4	17		0.340(12)	0.0014(2)	0.04425	0.73(7)	0.1
3.8	18+19		0.263(7)	0.00010(5)	0.01924	0.27(14)	0.7
5.0	20		0.174(14)	0.00000(8)	0.00150	0.0(30.)	0.4
2.7	21	1.0	0.405(25)	0.0042(3)	0.04478	2.09(14)	1.0
2.8	22		0.412(12)	0.0019(1)	0.03474	1.56(12)	0.3
2.85	23		0.393(14)	0.0012(1)	0.03059	1.31(30)	0.4

Table 3: Results for c_2, for the reduced string tension K_r and for K_r/Λ_F^2. The Λ_F-parameters are from eqn. (30).

Returning to table 3 and to $\xi^2 = 3/2$, we note that the drop of the ratio K_r/Λ_F^2 with increasing β is statistically perhaps only marginally significant, given the uncertainties in the subtraction of the perturbative term. The difference of this value between $\xi^2 = 3/2$ and $\xi^2 = 2/3$ taken at the resp. smallest β-values, is less dependent on the details of the subtraction, as the Λ_F-parameters are quite similar in this case. Thus the difference is more than a 20 st.d. effect, which should be taken seriously.

In the previous analysis, the extraction of K_r is based on the R-dependence of the potential at fixed β. A systematically and statistically independent method is to establish the existence of a non-perturbative term K_r from the β-variation. This is possible due to the large β-intervall covered by our data. For this purpose, the potential differences will be be represented, at given R and ξ, by the ansatz (see eq. (17))

$$\begin{aligned} V(R+a,\beta) - V(R,\beta) &= V_p(R+a) - V_p(R) \\ &\quad -\frac{C_r g_0'^2}{4\pi}\left(\frac{a_1(R)}{R} - \frac{a_1(R+a)}{R+a}\right) \\ &\quad +\frac{1}{R(R+1)}\sum_{i=2,4} v_{i,R}\alpha^i(R+a/2) \\ &\quad +\kappa_R \exp\left(-\gamma_R/g_0'^2\right). \end{aligned} \tag{30}$$

Here no corrections for R-dependent perturbative lattice artifacts to 1-loop order have been made, and we therefore expect the coefficients $v_{2,R}$ to be R-dependent. This is the case, and if we omit the tree-level artifacts in (31) and include a term with $i = 1$, the variation of $v_{1,R}$ nicely corresponds to the pattern of lattice artifacts. With all parameters free, the fit becomes unstable, but there are acceptable global fits with rather R-independent parameters $v_{i,R} = v_i$, $i = 3,4$, $\kappa_R = \kappa$ and $\gamma_R = \gamma$, where the higher order coefficients $v_{i,R}$, $i = 2,3,4$ are of $\mathcal{O}(1)$. As in [8] we find that γ is larger that predicted from asymptotic scaling, pointing towards linear term which vanishes in the continuum limit. This effect is, however, not very pronounced at $\xi^2 = 3/2$, in contrast to the case $\xi^2 = 2/3$. This is in agrement with the trend shown in table 3. The results for the reduced string tensions are now slightly R-dependent, but they are statistically perfectly consistent with those obtained by the fit at fixed β. Especially, the large discrepancy between $\xi^2 = 3/2$ and $\xi^2 = 2/3$ is fully reproduced for all R. Equally important is that, as in [8], a decent fit with enforcing $\kappa = 0$ is only possible with oscillating higher order coefficients $v_{i,R}$, $i = 2,3,4$ of $\mathcal{O}(10)$. This we regard as a typical consequence of an attempt to perform a power series expansion of a function with a large non-analytic term.

The violations of scaling between different values of ξ can be made visible more directly. We note that the cases $\beta = 2.2$, $\xi^2 = 3/2$ and $\beta = 3.4$, $\xi^2 = 2/3$ (data sets #1+#2 vs. #17) are closely related in the sense that the Λ_F-parameters are similar (see table 3, column 6). This similarity is based exclusively on the perturbative calculation of the ξ-dependent Λ_F-parameter. Using the ansatz (18) to correct for the small difference of the parameters, and of (16) to correct for lattice artifacts, the potentials can be compared directly. They have exactly the same curvature at small distances, but a huge linear difference, as shown in fig. 4 (upper points, empty circles). The same holds for the cases $\beta = 2.3$, $\xi^2 = 3/2$ vs. $\beta = 2.85$, $\xi^2 = 1$ (sets #4 vs. #23) and $\beta = 3.4$, $\xi^2 = 2/3$ vs. $\beta = 2.7$, $\xi^2 = 1$ (sets #17 vs. #21). Since now the β-values are larger and the difference in ξ^2 is smaller, the discrepancy is smaller.

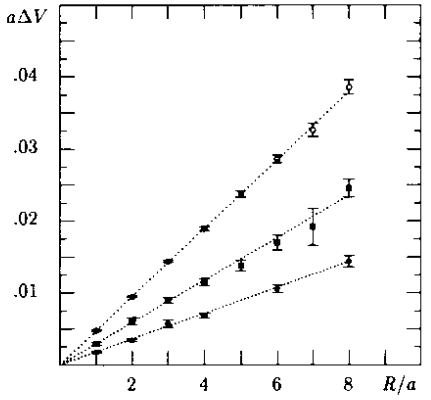

Figure 4: Difference between 3 pairs of potentials at similar Λ_F, namely data sets #1+#2 vs. #17 (open circles), data sets #17 vs. #21 (full boxes), and data sets #4 vs. #23 (full circles). Corrections for differences in Λ_F and for lattice artifacts have been made. The dotted lines are linear fits to the data.

In all three cases the perfect linearity of the difference gives excellent support for the interpolation formula (22).

It is less spectacular to compare cases where the forces agree in the 'linear' region. This holds true for $\beta = 2.2$, $\xi^2 = 3/2$ and $\beta = 3.3$, $\xi^2 = 2/3$, in spite of the fact that the reduced string tensions are quite different (see table 3, column 5). The forces agree nevertheless well for $R > 3a$, due to the different Λ_F-parameters. The latter circumstance, however, leads to a discrepancy in the force at $R/a = 1$, 2 and 3, which is of the order of 6% at $R/a = 1$ and which decreases quickly with increasing R. We do not plot these discrepancies as they are barely visible in a graphical representation of the force or of the effective coupling constant, but they are statistically highly significant. The discrepancies are slightly larger than the complete corrections for the lattice artifacts, which we believe to be well determined by the fits at large β (see next subsection).

4.3 More on Lattice Artifacts

The deviations of the perturbative lattice potential from the continuum form, beyond those on tree and 1-loop level, have been determined by hand, demanding agreement between the fit and the Monte Carlo data at $\beta = 2.8$, $\xi^2 = 3/2$ and at $\beta = 3.8$, $\xi^2 = 2/3$. This determination requires an assumption on the coefficient c_2 (see eq. (18) and table 3). This coefficient has been assumed to ly in the middle of a range which is determined in the following way.

If we choose a very low value of c_2, the $\mathcal{O}(g'^6)$-lattice artifacts have to be increased strongly, in order to simulate a Coulomb-like curve. Thus they begin to exceed the 1-loop artifacts given in table 1. At the same time, one needs a relativily larger value of K_r in order to compensate for the decrease of the quasi-linear rise of the perturbative potential at large R/a. Thus one will obtain a large value of K_r/Λ_F^2, exceeding that obtained at small values of β, although there the trend is still towards a decrease of

this ratio for increasing β. Specifically, for $c_2 \leq 0.2$ the lattice artifacts begin to look absolutely crazy.

If we increase c_2, the potential fit at $\beta = 2.8$, $\xi^2 = 3/2$ will increase too strongly at large R to allow for a positive linear term, without modifying again the lattice artifacts in an extreme way. Since we exclude a linearly falling non-perturbative piece on general grounds, this introduces a rather sharp upper limit of $c_2 \leq 0.5$ at $\beta = 2.8$. The analysis presented above is based on a value somewhere in the center of this window, namely $c_2 = 0.33$.

The crucial observation now is that if we repeat the analysis with values of c_2 at the above limits, the discrepancy between K_r/Λ_F^2 at $\xi^2 = 3/2$ and at $\xi^2 = 2/3$ does not change essentially. The difference between these values stays approximately constant, whereas the ratio is always larger than the value 2.5.

It has to be asked what kind of modifications of the artifacts are necessary in order to bring the results for K_r/Λ_F^2, as function of ξ^2, to mutual agreement. In order to achieve this, we have to choose different Λ_F-parameters. E.g., incresing Λ_F has a threefold effect:

- It trivially increases the denominator of K_r/Λ_F^2.
- It lowers K_r by subtracting a larger perturbative piece.,
- It leads to a different β-value to be compared with in the isotropic case.

These effects combine in such a way that a ξ^2-independent choice

$$\Lambda_F \approx 21.0\, \Lambda_{latt} \tag{31}$$

is appropriate to get a match, with respect to K_r/Λ_F^2, between the cases $\xi^2 = 3/2$ and $\xi^2 = 2/3$. This would imply imply that the Λ_F-parameter does not depend essentially on ξ, in contrast to the perturbative results. Of course, the modification of Λ_F induces variations in the interpolation ansatz (18) which have to be balanced by a modification of the artifacts. It turns out that for $\xi^2 = 3/2$, the artifact for the force at $R/a = 1$ has to be reduced by almost a factor 3, as compared to the case $\xi^2 = 2/3$, and it is much smaller than the tree level contribution. Also the pattern of the R-dependence is completely at variance with the 1-loop results shown in table 1. We believe these inconsistencies to be strong enough to rule out such modifications of the Λ_F-parameters.

5 Discussion and Conclusions

The analysis of the Monta Carlo data in the small R-region is based on the following two assumptions:

- The static potential $V(R)$, for fixed R as a function of β, can be expanded as a well convergent series in the renormalized coupling constant plus a non-perturbative term which is of the form (1).
- The non-perturbative term can be approximated, apart from an irrelevant constant, by a term linear in R. Its coefficient will be called the reduced string tension K_r.

The rather accurate data are perfectly consistent with this assumptions, whereas an attempt to set $K_r = 0$ will lead to a blow up of the higher order terms in the expansion of $V(R)$.

From column 7 of table 3 it is then apparent that K_r/Λ_F^2 shows the following departures from perturbative scaling:

- It drops for increasing β, for all three cases $\xi^2 = 3/2$, 1 and 2/3, i.e. asymptotic scaling does not hold.
- It varies by more than a factor 2.5 between the cases $\xi^2 = 3/2$ and $\xi^2 = 2/3$, if data sets with coinciding Λ_F-parameters are compared.

The first observation, which is not new, could be accommodated for by using a scaling function Λ_F (as function of the bare coupling constant g_0^2) which differs significantly from the 2-loop formula (14). The scale may essentially be determined by the potential slope in the linear region, since superficially the influence of the slope is much stronger than that of the logarithm in the region of small R (at least if one allows for significant errors in the lattice artifacts). At $\xi^2 = 3/2$, where the dependence of K_r/Λ_F^2 on β is weak, this imposes no significant difficulty on the choice of the potential parameters. At $\xi^2 = 2/3$ the situation is quite different, and a smooth ansatz for the scale parameter as a function of β, e.g. of the form

$$\Lambda_F = const(1 + \lambda/\beta)\Lambda_{latt}, \tag{32}$$

requires that the nonleading term is larger than the leading one in the present range of β. It furthermore seems to be difficult to find a convincing parametrization of lattice artifacts. The possibility to vary the scale parameter has been carefully studied also in pure SU(3) gauge theory. As mentioned in section 3.2, the Λ_F-parameter can be determined from an effective coupling constant $\alpha_{eff}(< P >)$ (P is the plaquette value), which in turn is derived from a comparison of the perturbative expansion of $\ln < P >$ (in terms of $\alpha_{eff}(< P >)$) with the Monte Carlo result [18, 22]. It had been shown previously in [23] that the departures from asymptotic scaling can be strongly reduced by this procedure. It should be noted, however, that they are not eliminated completely, and the differences in the scaling behaviour between string tension, ρ−mass and nucleon masses from Wilson and staggered fermions, which are not affected by a redefinition of the scale, are of the same order as the former quantity [23]. Furthermore, the distribution of the plaquette value P in the presently accessible region of β extents to such low (negative) values that a universal significance to the average value is difficult to understand. Although it has to be admitted that the variation of the scale as a function of the bare coupling constant is a complicated issue, all available information points towards a strong decrease of the non-perturbative effects for increasing β.

The dependence of the ratio K_r/Λ_F^2 on ξ is of different quality and cannot easily be accommodated for. The discrepancies are apparent both in the R-behaviour at fixed β and in the β-behaviour at fixed R. In the first case, one can compare potentials at (almost) coinciding scales, which are taken from perturbation theory. One finds that the curvatures of the potential are completely identical after very small corrections for scale differences and after subtraction of the lattice artifacts. The latter are taken from perturbation theory up to a higher order term which is determined at very large β. Its contribution to potential differences is at most 2%. In spite of the perfect match of the curvature, there is a large linear deviation between the potentials, with a clear trend in ξ^2: large ξ^2 imply a large linear difference. It is also possible to compare potentials which agree in their almost linear rise at large R. They show a clear discrepancy in the force at small R, which is larger than 6% between $R/a = 1$ and $R/a=2$, when the comparison is made between $\beta = 2.2$ ($\xi^2 = 3/2$) and $\beta = 3.3$ ($\xi^2 = 2/3$). One thus can state that for identical Coulomb-like forces the linear term may vary within a factor 3 for different actions.

In the second case, we find that the potential differences at fixed R can be expanded into a power series in the running coupling constant only at the expense of large and oscillating higher order terms, and that a decent expansion requires the inclusion of a non-perturbative term of the form (1). Its prefactor, as function of R, is constant within a reasonable accuracy, i.e. its contribution to the potential is linear. It agrees closely with the slope found in the R-dependent fit, especially with respect to the large discrepancy between $\xi^2 = 3/2$ and $\xi^2 = 2/3$.

We have studied two ways to modify the interpolation formula for the potential, in order to obtain a ratio K_r/Λ_F^2 independent of ξ. One way was a variation of the second order coefficient, along with appropriate modifications of the lattice artifacts. There was no significant change of the discrepancy. The other way was a shift of the Λ_F-parameter away from the perturbative prediction by an amount necessary to enforce agreement. We found the necessary modifications to be absolutely inconstistent with the trend of the one-loop perturbative calculations. Since the linear term seems to vanish in the approach to the continuum limit, especially in the case $\xi^2 = 2/3$, it is likely that it is simply a lattice artifact.

The consequence would be that lattice gauge theory does not support the bag picture, and that perturbation theory at small distances is valid without corrections from strings, membrane surfaces etc. The confining force would then arise by the necessary modification of perturbation theory for the Wilson loops, which is dictated by positivity.

As for the quantitative implications, we remark that, according to [6], in the isotropic case at $\beta = 2.85$ the full string tensions turns out to be $a^2K = 0.00401 \pm 0.0004$, whereas the reduced string tension K_r is, according to table 3, $a^2K_r = 0.0012 \pm 0.0001$. If we assume that K_r/Λ_F^2 vanishes in the continuum limit, the full string tension would be reduced by about 30% for $\beta \to \infty$. This is in qualitative agreement with the SU(3)-case [23], where the extrapolation has been performed numerically.

The consequences at finite distances depend on the physical scale. Following again the analysis of ref. [6], the distance of 8 lattice units at $\beta = 2.85$ corresponds to a physical distance of 0.23 Fermi. At this distance, the contribution from the reduced string tenstion in the isotropic case amounts to 14% of the total force. This percentage has to be regarded as a lower limit to the uncertainty of lattice results in the present region of β.

It remains to understand why e.g. an anisotropy with $\xi < 1$ leads to such a strong suppression of the reduced string tension. It is clear that in this case plaquettes with $\frac{tr}{2}\prod_{i\in p} U_i \ll 1$, pointing in space-space-directions, feel a suppression caused by the increased β-value which is necessary to match the perturbative region to the isotropic case. Now, it is a long-standing hypothesis [27, 28, 29] that a linear term in the potential is connected with the condensation of monopoles, which can be defined as three-cubes with an odd number of plaquettes with negative trace. If we inhibit the 'negative' plaquettes, we may well have killed the elementary monopoles, and this may be responsible both for the reduction of the linear term and for its steep decrease with β. Why the 'larger' monopoles do not survive, is an open question.

Acknowledgement

The authors want to thank the operation teams of the RS/6000-cluster at ISAM, IBM Heidelberg, of the Intel iPSC/860 and Paragon XP/S 10 at the HLRZ at KFA Jülich, and of the SP1 at IfH, DESY-Zeuthen, notably A. Fortenbacher, J. Docter, M. Weber, W. Friebel and R. Kowallik, for their excellent support over a long period. The grant of computer time by all three institutions is gratefully acknowledged. F.G. is grateful to ISAM, IBM Heidelberg for the hospitality extended to him. Discussions with H. Joos and M. Lüscher are gratefully acknowledged.

A Perturbation Theory on Anisotropic Lattices

A.1 The Zeroth-Order Action

On tree level, the expansion of the anisotropic action (3) in terms of the gauge fields follows the standard procedure. With the representation

$$U_\mu(x) = e^{ig_0 A^a_\mu(x)\tau_a/2}, \tag{33}$$

we obtain for a plaquette containing a time-like and a space-like link in direction i [8],

$$\begin{aligned} S_t &= \frac{\xi^2}{2}\sum_x \frac{tr}{2}\{\partial_0 A_i(x) - \partial_i A_0(x)\}^2 \\ &= -\frac{1}{2}\sum_x \frac{tr}{2}\{\xi^2 A_0(x)(\xi^2\partial_0^2 + \partial_i^2)A_0(x) + A_i(x)(\xi^2\partial_0^2 + \partial_i^2)A_i(x) \\ &\quad + (\xi^2\partial_0 A_0(x) + \partial_i A_i(x))^2\}. \end{aligned} \tag{34}$$

Adding a gauge fixing term under the trace,

$$(\partial_i A_i(x) + \xi^2\partial_0 A_0(x))^2, \tag{35}$$

to enforce the Feynman gauge, we arrive at the action (including now all plaquettes)

$$\begin{aligned} S_0 &= -\frac{1}{2}\sum_x \frac{tr}{2}\{\xi^2 A_0(x)(\xi^2\partial_0^2 + \sum_{j=1,3}\partial_j^2)A_0(x)\} \\ &\quad + \sum_{i=1,3} A_i(x)(\xi^2\partial_0^2 + \sum_{j=1,3}\partial_j^2)A_i(x). \end{aligned} \tag{36}$$

In order to get a more symmetric action, we first perform a change of variables for the time-like links:

$$U_0(x) = e^{ig_0 A^a_0(x)\tau^a/2} \to U'_0(x) = e^{ig_0 A'^a_0(x)\tau^a/2\xi}. \tag{37}$$

We remark that in expectation values, i.e. in ratios of functional integrals, the factor ξ for the differential cancels out on tree level. The corrections on 1-loop level will be discussed in the subsection 'Fadeev-Popov Ghost and Measure'.

The action is then

$$S_0 = -\frac{1}{2}\sum_x \frac{tr}{2}\{\sum_{i=1,3} A_i(x)\Delta_\xi A_i(x) + A'_0(x)\Delta_\xi A'_0(x)\}, \tag{38}$$

[8] We call this a **timelike** plaquette

where the anisotropic lattice Laplacian is given by

$$\Delta_\xi = \xi^2\partial_0^2 + \sum_{j=1,3}\partial_j^2. \tag{39}$$

The gauge fixing term now reads

$$S_{gf} = \frac{1}{2}(\xi_\mu\partial_\mu A'_\mu)^2, \quad \xi_\mu = \{\xi, 1, 1, 1\}. \tag{40}$$

In the following we shall drop the prime-symbol for A_0 again.

We next introduce the Fourier representation of the A_μ on an anisotropic lattice of size $V_\xi = \xi L \times L^3$:

$$A_\mu(x) = \frac{1}{V_\xi}\sum_n e^{ik_n x} A_{\mu,n}, \tag{41}$$

and obtain, for $L \to \infty$,

$$S_0 = \frac{1}{2}\int_{-\pi}^{+\pi}\frac{dk_0\, dk_i}{(2\pi)^4}\sum_\mu A_\mu(k)A_\mu(-k)(\xi^2\widehat{k_0}^2 + \sum_{i=1,3}\hat{k}_i^2). \tag{42}$$

The bare propagator is diagonal in space-time directions (due to the Feynman gauge), and its momentum part is

$$D_\xi(k) = 1/(\xi^2\widehat{k_0}^2 + \sum_{i=1,3}\hat{k}_i^2). \tag{43}$$

In order to gain insight into the ξ-dependence of e.g. logarithmic terms and to have approximate rotational invariance for numerical integrations, the transformation $k_0 \to k'_0/\xi$, (6) in section 1) is useful. It leads to the more isotropic propagator

$$D'_\xi(k') = 1/(\xi^2\widehat{k'_0/\xi}^2 + \sum_{i=1,3}\hat{k}_i'^2), \tag{44}$$

where $D'_\xi(k')$ as function of k'_0 differs from the isotropic case only to $\mathcal{O}k'^4_0$. Thus, apart from the extra factor ξ^{-1} in (6), one will get a different cut-off effect, i.e. a change in the Λ-parameter.

To fix the transition from the isotropic to the anisotropic case, one has to find out how many plaquettes are involved in the formation of the operator, which contributes to the potential. We note that all contributing plaquettes must be time-like to this order, since they must contain factors A'_0 which can be contracted with corresponding A'_0 in the external Wilson loops[9]. Then there is a factor ξ^2 for each plaquette, a factor $1/\xi$ for each A'_0, not only from the plaquettes but also from the external loop. Internal momenta integrations proceed according to 5. We now discuss the various contributions to the potential.

A.2 Expansion of the Wilson Loop

The contributions of the Wilson loop expansion to the potential will encounter a factor ξ^{-4} from the external Wilson loops, due to 4 external time-like vector potentials. The

[9] This is due to working in the Feyman gauge.

relevant integrals are thus

$$V_{WI}(R) = \lambda\xi^{-4}\left[\int_{\hat{q}}\widehat{Rq_1}^2\int_k D_\xi(q-k)\,|_{q_0=0}\,D_\xi(k)cos^2\tfrac{k_0}{2}/\widehat{k_0}^2\right. \quad (45)$$
$$-2\int_{\hat{q}}\widehat{Rq_1}^2 D_\xi(q)\int_k D_\xi(k)/\widehat{k_0}^2\,|_{q_0=0}$$
$$\left.+\tfrac{1}{3}\int_{\hat{q}}\widehat{Rq_1}^2 D_\xi(q)\,|_{q_0=0}\int_k D_\xi(k)\right],$$

with

$$\lambda = g_0^4 NC_R/4. \quad (46)$$

The integration contour at the singular point $k_0 = 0$ is in the lower half plane. Whereas the second and third terms are proportional to the tree level potential, there is a logarithmic contribution from the first one, which is, after the transformation (6), proportional to ξ^{-3}. There is no further change in the logarithm, since it is obtained by any finite integration interval around $k_0 = 0$, where $D'_\xi(k') = D_\xi(k) + Ok_0^4)$.

A.3 The Triple-Gluon Coupling

The triple gluon contribution arises from two time-like plaquette terms with at least two time-like vector potentials, which will be contracted with two time-like vector potentials on the Wilson loop. From these items, all ξ-factors cancel. The contribution to the potential is then of the form

$$V_{3g}(R) = \int_{\hat{q}}\widehat{Rq_1}^2 D_\xi^2(q)\sum_{i=1,4}\pi_i(q)\,|_{q_0=0} \quad (47)$$

where the $\pi_i(q)$ are various ξ-dependent contributions to the gluon propagator. We have

$$\pi_1 = 2\lambda\xi^{-2}\int_k\int_{k'}\delta(k+k'-q)D_\xi(k')(1-\frac{1}{4}\hat{k_0}^2) \quad (48)$$

which is independent of q. The factor ξ^{-2} is due to the fact that 4 time-like gauge fields from the expansion of the plaquettes contribute here. Next we have

$$\pi_2 = \lambda\int_k\int_{k'}\delta(k+k'-q)D_\xi(k)D_\xi(k')(\xi^{-2}(4-\widehat{k_0}^2)-\frac{1}{4}\widehat{2k_0}^2)\hat{q}^2 \quad (49)$$

The first term in the bracket gives a logarithmic contribution, yielding again a term proportional to ξ^{-3} after the substitution (6). The next term has no logarithmic singularity:

$$\pi_3 = -2\lambda\int_k\int_{k'}\delta(k+k'-q)D_\xi(k)D_\xi(k')\xi^{-2}(1-\frac{1}{4}\widehat{k_0}^2)\sum_{\mu=1,3}\widehat{q_\mu}^2\widehat{k_\mu}^2 \quad (50)$$

The last term,

$$\pi_4 = \frac{5}{2}\,lambda\int_k\int_{k'}\delta(k+k'-q)D_\xi(k)D_\xi(k')\widehat{2k_0}^2 \quad (51)$$

leads to a $1/(\hat{q}^2)^2-$singularity which is cancelled against a collection of terms, namely against π_1, terms from the four gluon coupling, from the Fadeev-Popov ghost and the measure contribution. The sum of these terms is, written in the form of (47),

$$\pi_c = -\frac{1}{5}\pi_4 - 2\lambda\int_k D_\xi^2(k)\widehat{k_0}^2. \quad (52)$$

The difference between (51) and (52) is a term $\sim \xi^{-3}\ln q^2/q^2$.

A.4 The Quadruple-Gluon Coupling

This contribution arises from a higher order expansion of a single plaquette term, and several ξ^2-factors have to be considered: The one in front of the plaquette (only time-like plaquettes contribute in Feynman gauge), those coming from time-like gauge potentials and those in the internal propagators. The main task is to keep track of the number of time-like gauge fields. The complicated result is, written again similar to (47),

$$\pi_{4g,a} = \frac{\lambda\xi^{-4}}{6}\left\{\hat{q}^2[\Delta_\xi(1+6\xi^2)-2\xi^2\Delta_{0,\xi}-\Delta_{1,\xi}/2]+3[\Delta_{1,\xi}-6\xi^2(2\Delta_\xi-\Delta_{0,\xi})]\right\}. \quad (53)$$

Here

$$\Delta_\xi = \int_k D_\xi(k), \quad (54)$$
$$\Delta_{0,\xi} = \int_k \widehat{k_0}^2 D_\xi(k), \quad (55)$$
$$\Delta_{1,\xi} = \int_k \widehat{k_1}^2 D_\xi(k). \quad (56)$$

The second bracket is essential to cancel the $1/\hat{q}^4$-singularity. We finally note that the fourth order expansion of the classical field tensor gives a term proportional to

$$\pi_{4g,b} = -\frac{2N^2-3}{N}\hat{q}^2\left[\xi^{-4}\Delta_{1,\xi}+\xi^{-2}\Delta_{0,\xi}(k)\right]. \quad (57)$$

A.5 The Fadeev-Popov Ghost and the Measure

For the calculation of the Fadeev-Popov-determinant (see [31]) one has to note that the gauge function according to (40) is $\xi-$dependent, and for the transformation of the gauge fields under local gauge transformations one has to take into account that the gauge fields in time-direction are A'_0/ξ. There is a second order term in the expansion of the logarithm in the formula for the determinant,

$$\pi_{FP,a} = -\frac{\lambda}{2}\int_k\int_{k'}\delta(k+k'-q)D_\xi(k)D_\xi(k')\widehat{2k_0}^2 \quad (58)$$

which can be combined with the last term from the 3-gluon coupling (51). The remaining term is independent of q,

$$\pi_{FP,b} = \lambda\xi^{-2}\Delta_{0,\xi} \quad (59)$$

which will be combined with the measure contribution to be discussed in the next paragraph.

For the measure, the correction for integrating over $dA_0^a, a = 1,2,3$ instead over dU_0 is found in the same way as in the isotropic case except that we have to take into account the substitution (refaprime). This gives a factor ξ^{-2}, and the same factor arises from contraction with the fields from the Wilson loop. We thus will get again a q-independent integral, written as a contribution to the gluon propagator in (47)

$$\pi_M = -\frac{\lambda\xi^{-4}}{6}\Delta_\xi. \quad (60)$$

which can be combined with (59).

B Computational Details

The large lattices used in this investigation can only be handled on modern parallel computers with distributed memory. The efficient parallelization of the simulation code is a problem of considerable interest. It has been solved by domain decomposition into four-dimensional cubes with boundary exchange by message passing for the update program. The Wilson loops were analyzed after a reshuffling of the lattice such that each processor owned complete planes. This avoids communication during the build-up of Wilson loops. To store a full configuration on one node is clearly not possible.

The development of the parallel code took place on the cluster of 8 processors (IBM RISC System/6000 model 550) at ISAM, Heidelberg. The production started on this cluster, with more data taken on the IBM 9076 SP1 with 10 nodes at the IfH, Zeuthen, on the iPSC/860 and on the Paragon XP/S, both at the ZAM, KFA Forschungszentrum Jülich. A sustained speed between 30 and 50 MFLOPS/node could be achieved on most machines, partly after coding some routines in assembler. For a pure overrelaxation step for one link on one node, the time needed was around 10μsec, including communication. This number corresponds to 48 MFLOPS per node. The best performance has been reached on the IBM 9076 SP2 with 7.6μsec per link and node. The performance losses due to communication were in the order of 25 %, where the effective bandwidths, i.e. those measured including the necessary packing and unpacking to and from arrays, were between 4 and 7 MByte/sec. These figures represent only a small fraction of the ideal bandwidths, and they imply that the reordering of data on the nodes is a major bottleneck for communication.

A more complete description of tuning steps and ultimate performance can be found in [32] and [33].

References

[1] P. Hasenfratz and J. Kuti, Physics Reports **C40** (1978) 75

[2] R.L. Jaffe and K. Johnson, Phys. Lett. **60B** (1976) 1934

[3] S.L. Adler, Phys. Rev. **D 23**, (1981), 2905
S.L. Adler and T. Piran, Rev. Mod. Phys. 56 (1984), 1

[4] H. Lehmann and T.T. WU, Nucl. Phys. **B237** (1984), 205

[5] E. Eichten, K. Gottfried, T. Kinoshita, K.D. Lane and T.M. Yan, Phys.Rev. **D21** (1980), 203

[6] S.P. Booth, A. Hulsebos, A.C. Irving, A. McKerrel, C. Michael, P.S. Spencer and P.W. Stephenson, Nucl. Phys. **B394** (1993), 509

[7] S.J. Perantonis and C. Michael, Nucl. Phys. **B** (Proc. Suppl.) 20, (1991) 177

[8] F. Gutbrod, Z. Phys. **C 37**, (1987), 143

[9] F. Karsch, Nucl. Phys. **B205**, (1982), 285

[10] I. Bender, T. Hashimoto, F. Karsch, V. Linke, A. Nakamura, M. Schiestl and I.O. Stamatescu, Nucl. Physics **B** (Proc. Suppl.) 20, (1991), 329

[11] P. Weisz, R. Wohlert, Nucl. Phys. **B236** (1984), 397

[12] U. Heller, F. Karsch, Nucl. Phys. **B251** (1985), 254

[13] E. Kovacs, Phys. Rev. **D25**(1981), 871

[14] A. Billoire, Phys. Lett. **104B** (1981), 472

[15] C. Michael, Phys. Lett. **283B** (1992) 103

[16] R. Sommer, Nucl. Phys **B411** (1994) 839

[17] G.S. Bali and K. Schilling, Phys. Rev. **D 47** (1993) 661

[18] T. Klassen, CLNS 94/1294, **hep-th**9408016, preprint Cornell, August 1994

[19] ALPHA collaboration, G. de Divitis et al., Universality and the approach to the continuum limit in lattice gauge theory, **hep-lat**/9411017, December 1994

[20] M. Lüscher, R. Sommer, P. Weisz and U. Wolff Nucl. Phys. **B389** (1993) 247

[21] C. Michael, preprint Liverpool LTH 340, **hep-lat**/9412032, December 1994

[22] G.P. Lepage and P.B. Mackencie, Phys. Rev. **D48** (1993), 2250

[23] A. Ukawa, Nucl. Phys. **B** (Proc. Suppl.) 30, (1993), 1

[24] J. Fingberg, Universality, Scaling and Topology with a Modified Lattice Action, **hep-lat**-9412094

[25] D. Daniel, A. Gonzáles-Arroyo and C.P. Korthals Altes, Phys. Lett. **B251** (1990), 559, and references quoted therein.

[26] G. Parisi, R. Petronzio, F. Rapuano, Phys. Lett. **128B** (1983), 418

[27] G. Mack and V.B. Petkova, Z. Phys. **C 12** (1982), 177

[28] E.T. Tomboulis, Phys. Rev. **D23** (1981), 2371, Nucl. Phys. **B** (Proc. Suppl.) 34 (1994), 192 and references quoted therein

[29] H. Shiba and T. Suzuki, Nucl. Phys. **B**(Proc. Suppl.) 34 (1994), 182

[30] P. Hasenfratz and A. Hasenfratz, Nucl. Phys. **B193**, (1981), 210

[31] B.E. Baaquie, Phys. Rev. **D16** (1977), 2612

[32] F. Gutbrod, N. Attig and M. Weber, The SU(2)-Lattice Gauge Theory Simulation Code on the Intel Paragon Supercomputer, KFA-ZAM-IB-9427, Jülich, November 1994, and to be published.

[33] P. Altevogt and F. Gutbrod, Monte Carlo Simulation of Lattice Gauge Theory on Multiprocessor Systems, Springer Lecture Notes in Computer Science 797 (ed. W. Gentsch, U. Harms), vol. I, (1994), 352